

PETROGRAPHY OF LUNAR METEORITE LAP 02205, A NEW LOW-TI BASALT POSSIBLY LAUNCH PAIRED WITH NWA 032. B. L. Jolliff, *R. A. Zeigler, and R. L. Korotev, Dept. of Earth and Planetary Sciences, Washington University, 1 Brookings Dr., Campus Box 1169, St. Louis MO, 63130; *zeigler@levee.wustl.edu.

Overview: Lunar meteorite LAP 02205 is a 1.23 kg basalt collected during the 2002 field season in the La-Paz ice field, Antarctica [1]. We present a petrographic description including mineral modes and compositions, and the major-element composition of the bulk meteorite. LAP 02205 is an Fe-rich, moderately low-Ti mare basalt that is similar in composition, mineralogy, and mineral chemistry to the NWA 032 basaltic lunar meteorite. LAP 02205 is yet another of the moderately low-Ti basaltic meteorites that are underrepresented among Apollo and Luna samples but that appear from remote sensing to be the most common basalt type on the Moon.

Methods: Mineral modes are estimated by image analysis of section LAP02005,33. Mineral and glass compositions were determined by electron microprobe analysis (EMPA; Table 1a), and major element chemistry was determined by a combination of instrumental neutron activation analysis (INAA; [2]) on rock chips and powders, and EMPA on fused beads (Table 1b).

Petrography: The LAP basaltic lunar meteorite has a coarse-grained, subophitic to intergranular texture and is composed predominantly of pyroxene (55%) and plagioclase (30%), with minor olivine (3%) and mesostasis dominated by ilmenite (5%), fayalite (5%), and cristobalite (2%). Spinel, troilite, Fe-Ni metal, chlorapatite, RE-merrillite, and basaltic glass (shock melt) occur in trace amounts. Pyroxene grains are anhedral, up to 1 mm in size, and are composites of pigeonite and subcalcic augite ranging in composition from $En_{2-5}Fs_{22-77}Wo_{11-36}$ (Fig. 1). Plagioclase typically occurs as elongated anhedral to subhedral grains up to 2 mm in length and displays a small compositional range ($An_{91-85}Or_{<2}$) and little zoning in individual plagioclase grains. Some of the plagioclase grains have been partially converted to maskelynite. Olivine phenocrysts are anhedral, up to 1 mm in size, show compositional zoning from Fo_{63-46} , and have melt inclusions and subhedral-euhedral chromite inclusions (Fig. 2). The main oxide in this basalt is

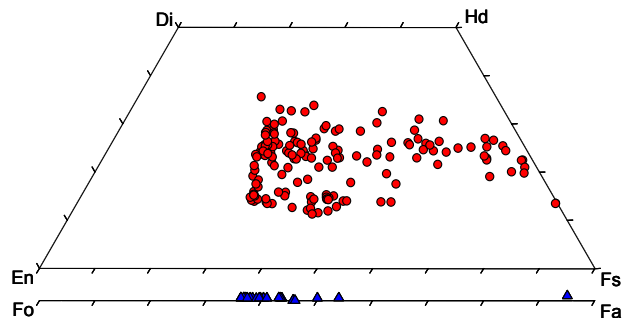


Fig. 1: Pyroxene (red circles) and olivine (blue triangles) compositions in LAP 02205,33

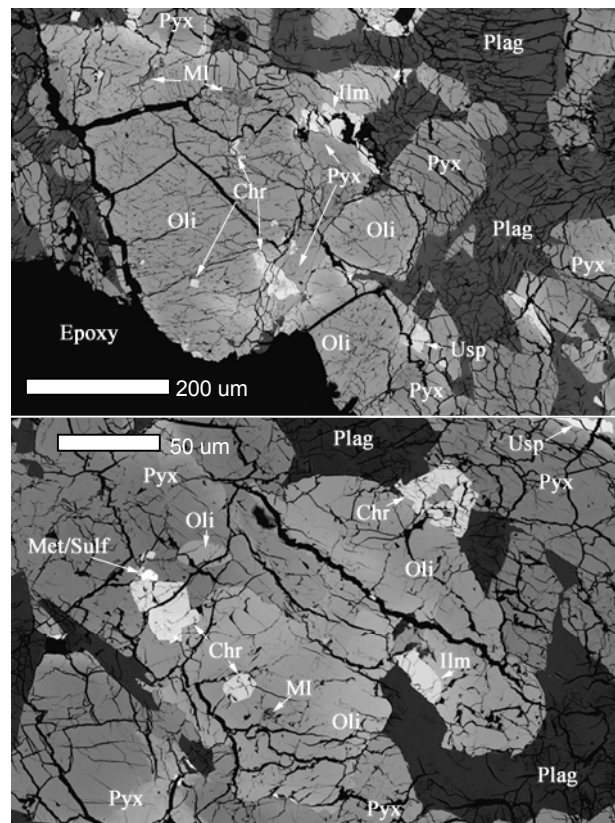


Fig. 2: (top) Backscattered electron (BSE) image of olivine (Oli) phenocryst surrounded by plagioclase (Plag) and pyroxene (Pyx). Chr=chromite; MI=melt inclusion; Ilm=ilmenite; Usp=ulvöspinel. (bottom) BSE image of olivine-pyroxene glomerocryst. Note intergrown Fe,Ni metal-sulfide grain (Met/Sulf).

Mg-poor ilmenite, which typically occurs as elongate laths and is associated with the mesostasis silica and fayalite. A few grains of more magnesian ilmenite are associated with the olivine phenocrysts. Spinel grains are less abundant, smaller ($< \sim 0.1$ mm), and range in composition from near endmember ulvöspinel to chromite. The mesostasis areas of this basalt consist chiefly of grains of cristobalite and fayalite, either together or separately, typically associated with ilmenite laths (Fig. 3). Cristobalite grains range in size up to ~ 0.5 mm, commonly have inclusions of K-feldspar and/or an incompatible-element-rich, ferroan glass, and occasionally are associated with grains of apatite or RE-merrillite. The fayalite grains (up to 0.75 mm) typically contain small grains of silica, plagioclase, and K-feldspar in a symplectic intergrowth. Trace amounts of troilite also occur in the mesostasis. A few grains of Fe metal are scattered through the sample. Several small areas of orange-brown glass with a bulk composition

approaching that of the bulk meteorite occur in thin section LAP02005,33.

Composition/Discussion: The partial maskelynitization of plagioclase, mosaic fractures in pyroxene, and presence of glass that appears to have formed by shock melting indicates that LAP 02205 experienced a shock pressure of ~30-35 GPa [3].

The bulk Mg' of LAP 02205 is 33 (Table 1b), which is lower than all of the Apollo and Luna basalts. The only lunar basalts that have a comparable Mg' are the lunar meteorites Asuka 881757 and Yamato 793169 [4]. On the basis of bulk chemical and mineral compositions, LAP 02205 is most similar to basaltic lunar meteorite NWA 032. The mineral assemblages and compositions for the NWA and LAP basaltic meteorites are similar, with pyroxene and olivine showing similar compositional ranges, although the LAP minerals extend to more ferroan compositions (NWA mineral compositions given by [5]). Plagioclase compositions are similar in An content, and differences in Fe and Mg reflect a faster cooling rate for NWA 032, consistent with textures. Oxides in both basalts include chromite early, with later ilmenite and ulvöspinel. The main differences are the higher modal abundance of olivine in NWA 032 (12% vs. 3%) and the presence of fayalite and cristobalite (= slower cooling) in LAP.

Although most of the differences in major and trace elements and olivine proportions between LAP 02205 and NWA 032 suggest a relationship by olivine fractionation, this is not supported by variations in Ti, K, and Ba, which are higher in NWA 032. Also, CaO is not as high in LAP 02205 as it should be following the appropriate amount of olivine fractionation. These characteristics suggest a more complex mechanism that may also have involved augite fractionation and segregation/loss of some late stage melt in LAP 02205, which is supported by the presence of an alkali-enriched mesostasis phase and relatively coarse-grained early-

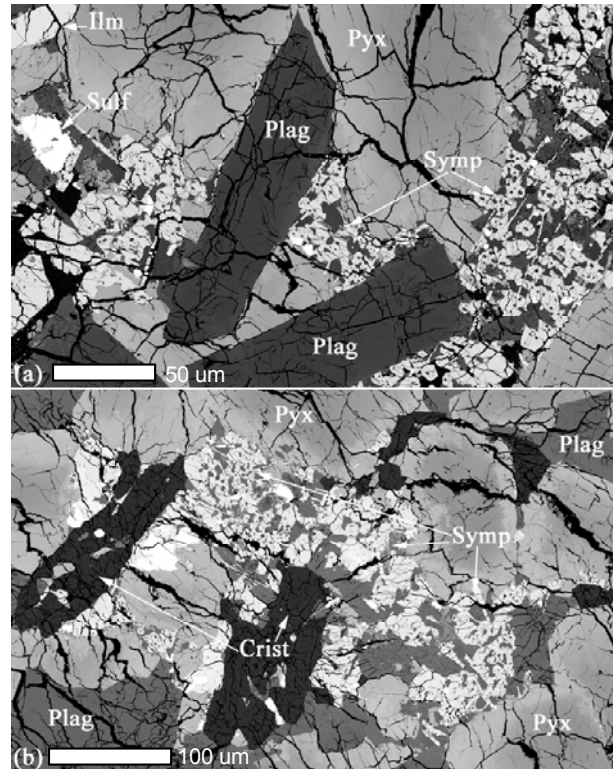


Fig. 3: BSE images of mesostasis. (a) Symplectite (Symp) areas are fayalite hosting plagioclase, silica, and K-feldspar. FOV = 0.6 mm. (b) Mesostasis with relatively coarse cristobalite (Crist), with inclusions of K-feldspar, fayalite, and ferroan residual-melt glass. FOV = 1 mm.

formed mineral assemblage. Otherwise, similar mineralogy, mineral chemistry, and trace-element signatures other than the alkalis [2] do support a relationship between NWA 032 and LAP02205.

References: [1] Antarctic Meteorite Newsletter 26, n2, Aug. 2003. [2] Korotev et al. (2004) *This Volume*. [3] Hörz et al. (1991) *Lunar Sourcebook*. [4] Korotev et al. (2003) *Ant. Meteor. Res.*, 152-175. [5] Fagan et al. (2002) *MAPS*, 37, 371-394. **Acknowledgements:** This work was supported by grant NAG5-10485 (L. Haskin).

Table 1a: Mineral Compositions in LAP02205,33

Mineral	Plag	Pig	Pig	Aug	Oli	Oli	Fa	Gls	Cri	Gls/kfs	Ilm	Usp
N	80	4	8	5	4	4	1	1	6	5	2	4
SiO ₂	47.2	45.3	51.7	49.5	36.6	34.6	29.8	46.3	98.0	77.7	0.02	0.08
TiO ₂	0.06	0.96	0.54	1.34	0.02	0.05	0.34	2.34	0.27	0.40	51.87	30.92
Al ₂ O ₃	33.3	0.95	1.31	3.07	<0.02	0.02	<0.02	13.9	0.73	10.8	0.10	2.13
Cr ₂ O ₃	0.02	0.05	0.59	0.91	0.28	0.16	<0.02	0.08	0.02	0.05	0.11	3.32
FeO	0.73	42.6	20.2	14.9	31.6	42.5	65.9	19.6	0.21	1.92	46.4	61.2
MnO	n.a.	0.52	0.36	0.29	0.34	0.48	0.65	0.22	n.a.	n.a.	0.40	0.35
MgO	0.21	0.68	18.7	13.8	30.8	22.0	1.77	3.45	0.02	<0.02	0.12	0.27
CaO	17.3	8.7	6.0	15.6	0.38	0.34	0.55	12.7	0.19	1.28	0.03	0.06
Na ₂ O	1.20	<0.02	<0.02	0.05	<0.02	<0.02	<0.02	0.51	0.13	0.16	<0.02	<0.02
K ₂ O	0.08	n.a.	n.a.	n.a.	n.a.	n.a.	<0.02	0.05	0.03	4.20	<0.02	<0.02
P ₂ O ₅	n.a.	n.a.	n.a.	n.a.	n.a.	n.a.	n.a.	n.a.	n.a.	n.a.	n.a.	n.a.
Sum	100.0	99.7	99.5	99.5	100.0	100.3	99.1	99.1	99.6	96.5	99.0	98.4
Mg'	34.3	2.8	62.3	62.3	63.5	48.0	4.6	23.9	11.9			
Fs:Fa:An	88.4	76.4	32.3	26.5	36.3	51.7	94.6					
Wo:Ca:Ab	11.1	21.4	14.2	29.7	0.6	0.5	1.0					
En:Fo:Or	0.5	2.2	53.4	43.8	63.1	47.8	4.5					

Italicized numbers determined by INAA, others by EMPA. 116 mg of LAP02205,20 and 125 mg of ,24 analyzed by INAA [2], and ~25 mg from each were used for fused-bead EMPA. Fs=ferrosilite, Fa=fayalite, An=anorthite, Wo=wollastonite, Ca=Ca-olivine component, Ab=albite, En=Enstatite, Fo=forsterite, Plag=plagioclase, Aug=augite, Pig= pigeonite, Cri=cristobalite, Kfs=K-feldspar, Gls=glass, N=number of EMPA analyses, n.a.=not analyzed, Mg'=Mg/(Mg+Fe)*100.

Table 1b: Bulk Composition

	,20	,24	Weighted
	58	66	Average
	45.9	45.7	45.8
	3.26	2.66	2.97
	9.93	9.81	9.88
	0.249	0.335	0.294
	22.7	22.3	22.5
	0.30	0.28	0.29
	11.1	11.2	11.1
	0.407	0.379	0.392
	0.07	<0.02	0.04
	0.09	0.08	0.09
	99.5	99.7	99.6
	30.3	35.6	32.9